Identifying the transverse and longitudinal modes of the K^* and K_1 mesons through their angular-dependent decay modes

In Woo Park[,1,*] Hiroyuki Sako,[2,†] Kazuya Aoki[,3,‡] Philipp Gubler[,2,§] and Su Houng Lee[1,‖]

[1]*Department of Physics and Institute of Physics and Applied Physics, Yonsei University, Seoul 03722, Korea*
[2]*Advanced Science Research Center, Japan Atomic Energy Agency, Tokai, Naka, Ibaraki 319-1195, Japan*
[3]*KEK, High Energy Accelerator Research Organization, Tsukuba, Ibaraki 305-0801, Japan*

Observing the mass shifts of chiral partners will provide invaluable insight into the role of chiral symmetry breaking in the generation of hadron masses. Because both the K^* and K_1 mesons have vacuum widths smaller than 100 MeV, they are ideal candidates for realizing mass shift measurements. On the other hand, the different momentum dependence of the longitudinal and transverse modes smear the peak positions. In this work, we analyze the angular dependence of the two-body decays of both the K^* and K_1. It is found that the longitudinal and transverse modes of the K^* can be isolated by observing the pseudoscalar decay in either the forward or perpendicular directions, respectively. For the K_1 decaying into a vector meson and a pseudoscalar meson, one can accomplish the same goal by further observing the polarization of the vector meson through its angular dependence on the two pseudoscalar meson decay.

I. INTRODUCTION

Understanding the generation of hadron masses stands as one of the fundamental puzzles in quantum chromodynamics (QCD). It is widely believed that spontaneous chiral symmetry breaking [1,2] partly contributes to the generation of hadronic masses [3–6]. Experiments conducted worldwide have aimed to observe the mass shift of hadrons at finite temperatures or densities [7–11]. This is because chiral symmetry is expected to be partially restored in the initial stages of relativistic heavy ion collisions and in nuclear matter probed by nuclear target experiments, respectively.

In particular, the J-PARC E16 experiment [8,12] will pursue the observation of the mass shift of the ϕ meson through e^+e^- pairs emanating from pA collisions. This measurement will be complemented by the J-PARC E88 experiment [13], which aims to measure the ϕ meson through its K^+K^- decay. The ϕ is expected to be a particularly sensitive probe, as its vacuum width is small,

meaning that any width increase in the medium will not be significant enough to disrupt experimental reconstruction of the peak position [14].

On the other hand, to isolate the effect of chiral symmetry restoration in a medium, the transformation of chiral partners toward degeneracy would be a critical experimental signal. This inevitably leads us to study the K^*, K_1 system as they appear to be the only realistically observable chiral partners, of which both have small vacuum widths [15,16].

The existence of the spin degrees of freedom, however, makes the situation more complicated, as both vector and axial vector mesons will have different responses depending on their spin orientation with respect to their motion relative to the medium. This effect is dominated by non-chiral symmetry-breaking effects [17], but it will cause the longitudinal and transverse modes to diverge for larger momenta, obscuring the peak position [18,19].

In a recent publication [20], we have shown that the longitudinal and transverse modes of the ϕ meson can be discriminated by analyzing the angular dependence of its two-body decay. In particular, the e^+e^- and K^+K^- decays can be used as complementary measurements.

In this work, we analyze the angular dependence of the two-body decays of both the K^* and K_1. As we will show, the longitudinal and transverse modes of the K^*, or any other vector meson such as the ρ (which decays from K_1) can be isolated by observing the pseudoscalar decay in either the forward or perpendicular directions, respectively. For the K_1 decaying into a vector meson and a pseudoscalar meson, one can accomplish the same goal by further

*darkzero37@naver.com
†hiroyuki.sako@j-parc.jp
‡kazuya.aoki@kek.jp
§philipp.gubler1@gmail.com
‖suhoung@yonsei.ac.kr
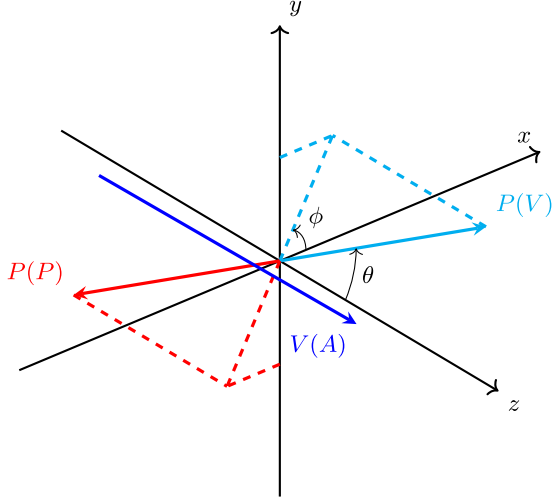
FIG. 1. Spin-1 particle decay in its rest frame. Cyan and red arrows each denote one decay particle after decay. The blue arrow stands for the traveling direction of the (axial) vector-meson in the Lab frame.

observing the polarization of the vector meson as discussed before.

The paper is organized as follows. In Sec. II, we introduce the relevant effective interaction Lagrangians and estimate the coupling constants for each decay. Then we study a spin-1 particle state with a superposition of three different helicities and discuss how the general angular distribution is connected to the spin density matrix. We furthermore point out that the same result can be obtained using the helicity formalism. We then summarize our discussion in Sec. III. More details regarding the calculations are provided in the appendices.

II. (AXIAL)VECTOR MESON DECAY RATE

In this section, we will introduce the basic kinematics of the two-body decay channels, along with phenomenological Lagrangians describing the interactions between the relevant particles, and estimate the corresponding hadronic coupling constants. We closely analyze the decay channels $\rho(770) \to \pi\pi$ and $K^*(892) \to K\pi$, both of which will be denoted as $V \to PP$. For the $A \to VP$ decays, we study $K_1(1270) \to \rho(770)K$ and $K_1(1270) \to K^*(892)\pi$. Here P denotes a pseudoscalar meson while V and A denote a vector meson and an axial vector meson, respectively. In the decay, we will denote θ and ϕ as polar and azimuthal angles of one of the decay products, measured in the center of mass (c.m.) frame (see Fig. 1). The z-axis is defined to align with the momentum direction of the initial particle in the Lab frame.

We assume that the initial (axial)vector meson is a superposition of the different helicity states $|\lambda\rangle$ ($\lambda = \pm 1$: transverse polarization, $\lambda = 0$: longitudinal polarization) with respective amplitudes a_λ. We can hence express the

general (axial)vector meson state as

$$|V/A\rangle = \sum_{\lambda=\pm 1,0} a_\lambda |\lambda\rangle. \tag{1}$$

The spin density matrix $\rho_{\lambda\lambda'}$ is defined using the coefficients a_λ and reads

$$\rho_{\lambda\lambda'} = a_\lambda a_{\lambda'}^\star. \tag{2}$$

The trace of the spin density matrix is normalized to 1: $\rho_{11} + \rho_{00} + \rho_{-1-1} = 1$. For a transversely polarized (axial) vector meson, the meson spin z component will be $J_z = \pm 1$, thus $\rho_{00} = 0$. In contrast, if the meson is longitudinally polarized, $J_z = 0$ and $\rho_{00} = 1$. The density matrix of an unpolarized meson has diagonal entries of $1/3$, specifically $\rho_{11} = \rho_{00} = \rho_{-1-1} = \frac{1}{3}$.

A. $\rho \to \pi\pi$ and $K^* \to K\pi$ decay

The phenomenological interaction Lagrangians of the vector meson with two pseudoscalar mesons used in this work, are adapted from Ref. [21] and given as

$$\mathcal{L} = g_{\rho\pi\pi}(\pi^+ \overset{\leftrightarrow}{\partial}_\mu \pi^- \rho_0^\mu + \pi^+ \overset{\leftrightarrow}{\partial}_\mu \pi^0 \rho_-^\mu + \pi^- \overset{\leftrightarrow}{\partial}_\mu \pi^0 \rho_+^\mu), \tag{3}$$

$$\mathcal{L} = \sqrt{2} g_{K^*K\pi}(\bar{K}\,\vec{\tau}\cdot\partial_\mu\vec{\pi} - \partial_\mu\bar{K}\,\vec{\tau}\cdot\vec{\pi})K^{*\mu}. \tag{4}$$

K^*, K are isomultiplets, their matrix representation being listed in Appendix A. $\overset{\leftrightarrow}{\partial}_\mu$ is defined as $\pi^+ \overset{\leftrightarrow}{\partial}_\mu \pi^- = \pi^+(\partial_\mu\pi^-) - (\partial_\mu\pi^+)\pi^-$. All the masses of isomultiplets are isospin averaged using the PDG data [22], giving $m_K = 495.644$ MeV, $m_{K^*} = 893.61$ MeV, $m_\rho = 775.16$ MeV and $m_\pi = 138.037$ MeV. Similarly, in order to evaluate the coupling constants $g_{\rho\pi\pi}$ and $g_{K^*K\pi}$, we use the partial decay width from the PDG [22]. The initial spin average involves a total of 3 degrees of freedom. For $\rho \to \pi\pi$, depending on the isospin, the decay modes are $\rho^+ \to \pi^+\pi^0, \rho^- \to \pi^-\pi^0$ and $\rho^0 \to \pi^+\pi^-$. For the $K^* \to K\pi$ decay, they are $K^{+*} \to K^+\pi^0, K^0\pi^+$ and $K^{0*} \to K^0\pi^0$, $K^+\pi^-$. Therefore, after summing over the initial isospin components, the average is obtained by dividing by a factor of 3 for $\rho \to \pi\pi$ and 4 for $K^* \to K\pi$. The respective widths are then obtained as

$$\Gamma_{\rho\pi\pi} = \frac{g_{\rho\pi\pi}^2}{8\pi}\frac{|\boldsymbol{p_1}|}{m_\rho^2}\frac{4}{3}|\boldsymbol{p_1}|^2 = 149 \text{ MeV},$$

$$\Gamma_{K^*K\pi} = \frac{g_{K^*K\pi}^2}{8\pi}\frac{|\boldsymbol{p_1}|}{m_{K^*}^2}4|\boldsymbol{p_1}|^2 = 51.4 \text{ MeV}, \tag{5}$$

where

$$|\boldsymbol{p_1}| = \frac{1}{2m_0}\sqrt{(m_0^2 - (m_1 - m_2)^2)(m_0^2 - (m_1 + m_2)^2)}$$

TABLE I.   Coupling constant for each decay channel and the respective momentum of the daughter particle in the c.m. frame.

Decay	$\rho \to \pi\pi$	$K^* \to K\pi$	$K_1 \to \rho K$	$K_1 \to K^*\pi$
$\vert\boldsymbol{p_1}\vert$(MeV)	362	289	27	299
g_{ABC}	5.96	3.27	3.26	0.71

is the momentum of the two produced particles in the c.m. frame, while m_0 stands for the mass of the initial particle. For the $V \to PP$ decay, m_1 is taken to be one of the outgoing π mesons. For the $A \to VP$ decay, m_1 is the mass of the produced vector-meson. From the partial decay width of the initial vector-meson, we can obtain the coupling strength of each decay channel. The resultant coupling constants of the respective interaction Lagrangians are listed in Table I.

Assuming that the initial (axial)vector-meson is in the general configuration of Eq. (1), we can obtain the general angular distribution as [23]

$$\frac{1}{\Gamma}\frac{d\Gamma}{d\Omega} = \frac{3}{8\pi}(2\rho_{00}\cos^2\theta + (1-\rho_{00})\sin^2\theta$$
$$- 2\mathrm{Re}[\rho_{1-1}]\sin^2\theta\cos 2\phi + 2\mathrm{Im}[\rho_{1-1}]\sin^2\theta\sin 2\phi$$
$$- \sqrt{2}\mathrm{Re}[\rho_{10} - \rho_{-10}]\sin 2\theta\cos\phi$$
$$+ \sqrt{2}\mathrm{Im}[\rho_{10} + \rho_{-10}]\sin 2\theta\sin\phi), \qquad (6)$$

where θ and ϕ are as before the polar and azimuthal angles of the outgoing daughter particle. The details of this calculation are given in Appendix B. Integrating $\frac{1}{\Gamma}\frac{d\Gamma}{d\Omega}$ over ϕ, we acquire the polar angle distribution as

$$W(\theta) = \frac{3}{4}((1-\rho_{00}) + (3\rho_{00} - 1)\cos^2\theta). \qquad (7)$$

If we substitute $\rho_{00} = 0$, $W(\theta)$ becomes the decay distribution of a transversely polarized (axial)vector meson, while for $\rho_{00} = 1$, we get its longitudinal counterpart. Both distributions are depicted in Fig. 2, where $\rho_{00} = 0$ (T) and $\rho_{00} = 1$ (L) correspond to the solid and dotted lines, respectively. They are also a depiction of Eq. (B3) in Appendix B. These results agree with the result derived using polarization tensor [20].

B. $K_1 \to \rho K$ and $K_1 \to K^*\pi$ decay

The Lagrangian characterizing the coupling between the axial vector meson and a vector and pseudoscalar meson [21] is given as

$$\mathcal{L} = \sqrt{2}m_{K_1}(g_{K_1\rho K}\bar{K}\vec{\tau}\cdot\vec{\rho}_\mu - g_{K_1 K^*\pi}\bar{K}^*_\mu\vec{\tau}\cdot\vec{\pi})K_1^\mu. \quad (8)$$

The matrix representation of the K_1 field is given in Appendix A.

As before, we first compute the partial decay widths using the above interactions, giving

$$\Gamma_{K_1\rho K} = \frac{g^2_{K_1\rho K}}{8\pi}|\boldsymbol{p_1}|\left(3 + \frac{|\boldsymbol{p_1}|^2}{m_\rho^2}\right) = 34.2 \text{ MeV},$$

$$\Gamma_{K_1 K^*\pi} = \frac{g^2_{K^*K\pi}}{8\pi}|\boldsymbol{p_1}|\left(3 + \frac{|\boldsymbol{p_1}|^2}{m_{K^*}^2}\right) = 18.9 \text{ MeV}. \quad (9)$$

The partial decay widths of the K_1 decay channels are taken from the PDG [22]. Following the same procedure as in the previous subsection, the angular dependence of the decay distribution is obtained as

$$\frac{1}{\Gamma}\frac{d\Gamma}{d\Omega} = \frac{3}{4\pi(3 + \frac{p_1^2}{m_1^2})}\left(1 + \frac{p_1^2}{2m_1^2}(1 - \rho_{00} + (3\rho_{00} - 1)\cos^2\theta\right.$$
$$- \sqrt{2}\mathrm{Re}[\rho_{10} - \rho_{-10}]\sin 2\theta\cos\phi$$
$$+ \sqrt{2}\mathrm{Im}[\rho_{10} + \rho_{-10}]\sin 2\theta\sin\phi$$
$$\left. - 2\mathrm{Re}[\rho_{1-1}]\sin^2\theta\cos 2\phi + 2\mathrm{Im}[\rho_{1-1}]\sin^2\theta\sin 2\phi)\right).$$
$$(10)$$

Integrating over ϕ, we now find the polar angle distribution for $K_1 \to \rho K(K^*\pi)$,

$$W(\theta) = \frac{3}{2(3 + \frac{p_1^2}{m_1^2})}\left(1 + \frac{p_1^2}{2m_1^2}(1 - \rho_{00} + (3\rho_{00} - 1)\cos^2\theta)\right).$$
$$(11)$$

As one can see, compared to Eq. (7) for the K^* decay, there is an extra momentum dependence in the second term inside the large bracket of the above equation. The angular dependence of this distribution is shown in Fig. 3. Unfortunately, unlike the case shown in Fig. 2, if the polarization of the final vector-meson is not measured, one cannot distinguish L or T mode of the initial K_1, which can be understood from the suppression factor $p_1^2/(2m_1^2) = 6 \times 10^{-4}$ $(\rho K), = 5.6 \times 10^{-2}$ $(K^*\pi)$ appearing in the second term in the large bracket of Eq. (11).

However, if one measures the polarization of the final vector meson, one can distinguish the T or L modes of the initial K_1 meson. Then, there are a total of four possible combinations of initial and final vector-meson polarizations. Explicit calculations of the corresponding four amplitudes are given in Appendix B. The final results are listed below.

(a)

(b)
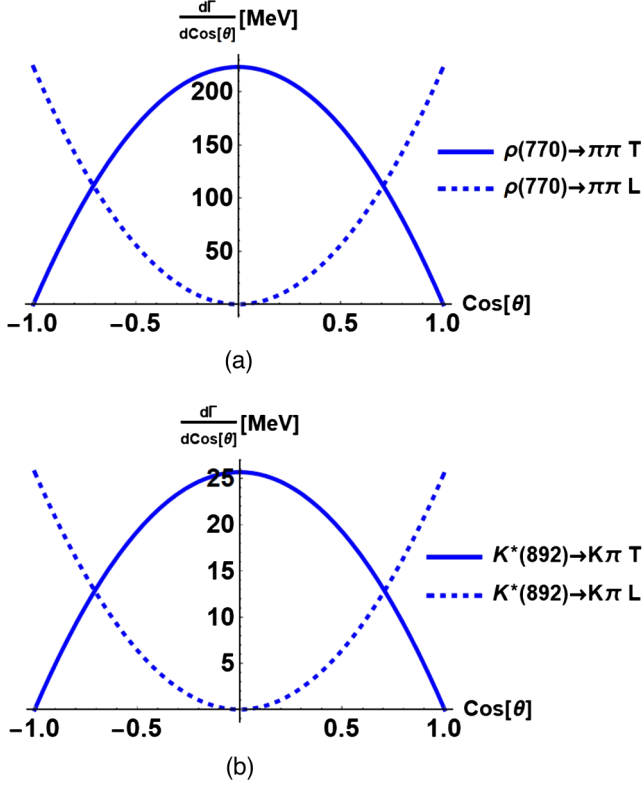
FIG. 2.   Angular distribution of decay rate of (a) $\rho \to \pi\pi$ and (b) $K^* \to K\pi$ in the c.m. frame for each polarization. T stands for transverse polarization and L stands for longitudinal polarization of the initial vector-meson. (a) $\frac{d\Gamma}{d\cos\theta}$ of $\rho \to \pi\pi$ in the c.m. frame and (b) $\frac{d\Gamma}{d\cos\theta}$ of $K^* \to K\pi$ in the c.m. frame.

$$|\mathcal{M}_{TT}|^2 = 2m_{K_1}^2 g_{K_1VP}^2 (1 + \cos^2\theta),$$
$$|\mathcal{M}_{LT}|^2 = 2m_{K_1}^2 g_{K_1VP}^2 \sin^2\theta,$$
$$|\mathcal{M}_{TL}|^2 = 2m_{K_1}^2 g_{K_1VP}^2 \frac{E_1^2}{m_1^2}\sin^2\theta,$$
$$|\mathcal{M}_{LL}|^2 = 2m_{K_1}^2 g_{K_1VP}^2 \frac{E_1^2}{m_1^2}\cos^2\theta. \qquad (12)$$

The first and second subscripts of $\mathcal{M}$ (T or L) here represent the polarization of an initial K_1 and final
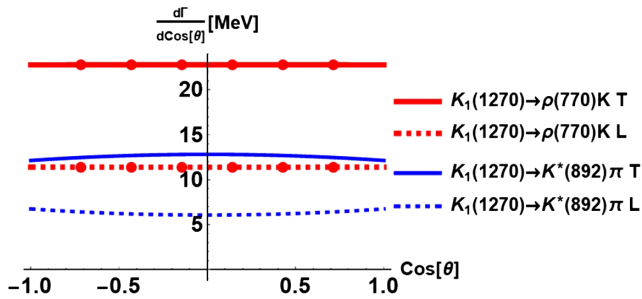
FIG. 3.   Angular decay distribution of the $K_1 \to \rho K$ and $K_1 \to K^*\pi$ channels in the c.m. frame for an initially polarized K_1.

vector-meson, respectively. The corresponding results are shown in Fig. 4. As can be seen there, once we isolate the angular dependence of T and L modes of the final vector meson, one can distinguish the transverse K_1 component by looking at the forward or backward direction. Conversely, when we measure the longitudinal component of the final vector meson, one can isolate the longitudinal K_1 component by again looking at the forward or backward direction. The improvement compared to the situation shown in Fig. 3 is clear.

C. Helicity basis and Wigner D-matrix

So far, we have computed the general angular decay distribution by using the respective interaction Lagrangian for each decay channel. Here, we shall see that the same angular distribution is reproduced by taking advantage of the helicity formalism. As the basic ingredient, we need the Wigner D-matrix and the density matrix of an initial (axial)vector-meson. The convention for the Wigner D-matrix [24,25] is adopted from that of Refs. [26,27]. The helicity basis for a massive particle is labeled by its momentum $\boldsymbol{p}$ and helicity λ and is obtained by a boost along z-direction from the rest state followed by the rotation described by an Euler angle $(\phi, \theta, 0)$.

(a)

(b)
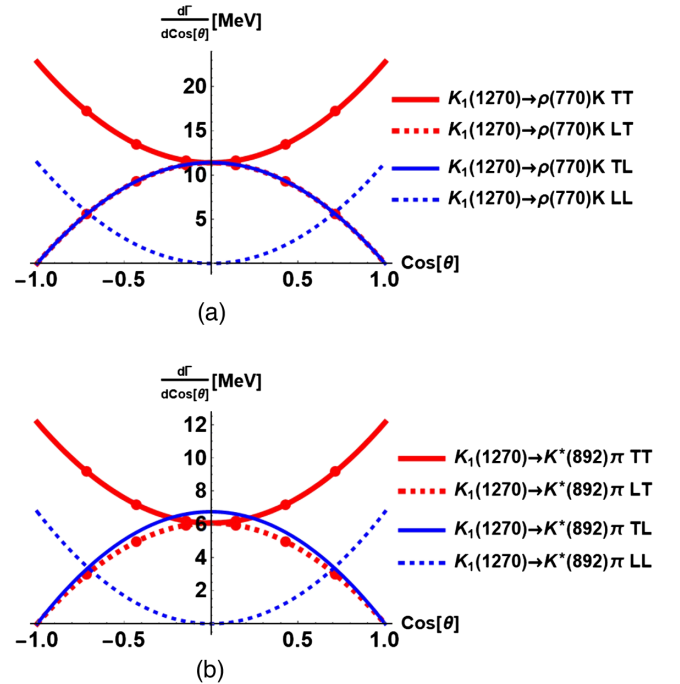
FIG. 4.   Angular distribution of decay rate of (a) $K_1 \to \rho K$ and (b) $K_1 \to K^*\pi$ in the c.m. frame for each polarization. The first and second T/L stands for the initial and final polarization of the spin-1 particle, respectively. (a) $\frac{d\Gamma}{d\cos\theta}$ of $K_1 \to \rho K$ in the c.m. frame and (b) $\frac{d\Gamma}{d\cos\theta}$ of $K_1 \to K^*\pi$ in the c.m. frame.

$$\mathcal{D}^1_{mm'}(\phi,\theta,0) = \begin{pmatrix} \frac{1+\cos\theta}{2}e^{-i\phi} & -\frac{1}{\sqrt{2}}\sin\theta e^{-i\phi} & \frac{1-\cos\theta}{2}e^{-i\phi} \\ \frac{1}{\sqrt{2}}\sin\theta & \cos\theta & -\frac{1}{\sqrt{2}}\sin\theta \\ \frac{1-\cos\theta}{2}e^{i\phi} & \frac{1}{\sqrt{2}}\sin\theta e^{i\phi} & \frac{1+\cos\theta}{2}e^{i\phi} \end{pmatrix},$$

$$\tag{13}$$

By applying a Wigner D-matrix, we rotate the density matrix so that the quantization axis rotates from the z-axis to align with the direction of momentum of an outgoing particle, specified by the angles ϕ and θ.

$$\left(\frac{1}{\Gamma}\frac{d\Gamma}{d\Omega}\right) = \frac{3}{4\pi}\sum_{\lambda,m,m'=\pm1,0} D^{1\dagger}_{\lambda m}\rho_{mm'}D^1_{m'\lambda}|H(\lambda_1,\lambda_2)|^2, \tag{14}$$

Here, $\lambda = \lambda_1 - \lambda_2$, where λ_1 and λ_2 are the helicities of the daughter particles of mass m_1 and m_2, respectively. $H(\lambda_1,\lambda_2)$ here stands for the interaction Hamiltonian for each helicity component of corresponding decay, which we can calculate from the interaction Lagrangians given before. More details regarding this calculation are explained in Appendix C. Since the final particles are spinless, for the $V \to PP$ decay for example one should use Eq. (14) with only the $\lambda = 0$ component by definition. This exactly reproduces the result of Eq. (6). On the other hand, for $A \to VP$ one needs to sum over all the helicity components $\lambda = \pm1, 0$.

III. SUMMARY AND CONCLUSIONS

In this work, we have shown that one can isolate the initial longitudinal and transverse modes of the K^* and K_1 from observing the decay angles and polarizations of their decay particles. In particular, for K^*, this is possible by measuring the decay angle distributions of the outgoing pseudoscalar mesons. For K_1, one furthermore needs to

determine the polarization of the outgoing vector meson to disentangle the longitudinal and transverse modes.

Such a measurement should be feasible in a future J-PARC experiment. This will help to reduce the uncertainty of the mass shift measurement of these two particles in nuclear matter. Once this is realized, the chiral partner nature of K^* and K_1 may be experimentally confirmed, which will bring us one step closer to understanding the role of chiral symmetry breaking and restoration to the generation of hadron masses.

APPENDIX A: EFFECTIVE INTERACTION LAGRANGIAN

K, K^*, and K_1 isodoublet matrices are defined as

$$K^* = \begin{pmatrix} K^{+*} \\ K^{0*} \end{pmatrix}, \qquad \bar{K} = (K^- \quad \bar{K}^0),$$

$$K_1 = \begin{pmatrix} K_1^+ \\ K_1^0 \end{pmatrix}, \qquad \bar{K}^* = (K^{-*} \quad \bar{K}^{0*}). \tag{A1}$$

Direct matrix multiplication yields the interaction Lagrangian as

$$\mathcal{L}_{\rho\pi\pi} = g_{\rho\pi\pi}((\pi^+\partial_\mu\pi^- - \partial_\mu\pi^+\pi^-)\rho^{0\mu} + (\pi^-\partial_\mu\pi^0 - \partial_\mu\pi^-\pi^0)\rho^{+\mu} + (\pi^+\partial_\mu\pi^0 - \partial_\mu\pi^+\pi^0)\rho^{-\mu}), \tag{A2}$$

$$\begin{aligned} \mathcal{L}_{K^*K\pi} = g_{K^*K\pi}[&\sqrt{2}(K^-\partial_\mu\pi^0 - \partial_\mu K^-\pi^0 + \bar{K}^0\partial_\mu\sqrt{2}\pi^- - \partial_\mu\bar{K}^0\sqrt{2}\pi^-)K^{+*\mu} \\ &+ \sqrt{2}(K^-\partial_\mu\sqrt{2}\pi^+ - \partial_\mu K^-\sqrt{2}\pi^+ - \bar{K}^0\partial_\mu\pi^0 + \partial_\mu\bar{K}^0\pi^0)K^{0*\mu}], \end{aligned} \tag{A3}$$

$$\begin{aligned} \mathcal{L}_{K_1VP} = &m_{K_1}g_{K_1K^*\pi}\sqrt{2}[(K_\mu^{-*}\pi^0 + \bar{K}_\mu^{0*}\sqrt{2}\pi^-)K_1^{+\mu} + (K_\mu^{-*}\sqrt{2}\pi^+ - \bar{K}_\mu^{0*}\pi^0)K_1^{0\mu}] \\ &- m_{K_1}g_{K_1\rho K}\sqrt{2}[(K^-\rho_\mu^0 + \bar{K}^0\sqrt{2}\rho_\mu^+)K_1^{+\mu} + (K^-\sqrt{2}\rho_\mu^+ - \bar{K}^0\rho_\mu^0)K_1^{0\mu}]. \end{aligned} \tag{A4}$$

APPENDIX B: DISENTANGLING THE POLARIZATIONS OF A VECTOR-MESON USING THE POLARIZATION TENSOR AND VECTOR

In this appendix, we will discuss two methods to disentangle the contributions of different polarization components of vector mesons to their decay amplitudes. The first one makes use of the polarization tensor and can only be used for purely transversely or longitudinally polarized vector/axial-vector mesons. The second more general method uses the polarization vector and can be applied to an arbitrary spin configuration. For the first method, we first need to define the polarization tensors as

$$P_T^{\mu\nu} = \begin{pmatrix} 0 & 0 \\ 0 & \delta^{ij} - \frac{q^i q^j}{\boldsymbol{q}^2} \end{pmatrix}, \qquad P_L^{\mu\nu} = \begin{pmatrix} \frac{\boldsymbol{q}^2}{m_0^2} & \frac{q_0 q^i}{m_0^2} \\ \frac{q_0 q^i}{m_0^2} & \frac{q_0^2 q^i q^j}{m_0^2 \boldsymbol{q}^2} \end{pmatrix}. \quad (B1)$$

Contracting these polarization tensors with the decay amplitude, we can disentangle its transverse and longitudinal parts. m_0, q_0 and q^i here stand for the mass, energy and momentum of the considered vector/axial-vector meson. In what follows, we will display the $\rho \to \pi\pi$ decay as an example of $V \to PP$ and the $K_1 \to \rho K$ decay as an example of $A \to VP$. The same method can also be applied to $K^* \to K\pi$ and $K_1 \to K^*\pi$, respectively. The decay amplitudes for the two cases are obtained as

$$\mathcal{M}_{\mu\nu} = g_{\rho\pi\pi}^2 (p_1 - p_2)_\mu (p_1 - p_2)_\nu,$$
$$\mathcal{M}_{\mu\nu} = 2m_{K_1\rho K}^2 g_{K_1\rho K}^2 \varepsilon_\mu(\lambda_\rho)\varepsilon_\nu^*(\lambda_\rho). \quad (B2)$$

Contracting these with the above polarization tensors, taking the final spin sum (if applicable), we get

$$\rho \to \pi + \pi \begin{cases} |\mathcal{M}|_T^2 &= 2g_{\rho\pi\pi}^2 \boldsymbol{p}_1^2 \sin^2\theta, \\ |\mathcal{M}|_L^2 &= 4g_{\rho\pi\pi}^2 \boldsymbol{p}_1^2 \cos^2\theta, \end{cases} \quad (B3)$$

and

$$K_1 \to \rho + K \begin{cases} |\mathcal{M}|_T^2 = m_{K_1}^2 g_{K_1\rho K}^2 \left(2 + \frac{\boldsymbol{p}_1^2}{m_\rho^2}\sin^2\theta\right), \\ |\mathcal{M}|_L^2 = 2m_{K_1}^2 g_{K_1\rho K}^2 \left(1 + \frac{\boldsymbol{p}_1^2}{m_\rho^2}\cos^2\theta\right). \end{cases} \quad (B4)$$

The different factors 2 and 1 appearing in the fist terms within the large brackets in Eq. (B4) are due to the different degeneracy factors of the two transverse and one longitudinal modes for a massive spin-1 particle.

Let us next move on to the second method, in which we can further study the contributions of the different helicity states and their mixing. The polarization vectors of the initial particle in its own rest frame for each helicity state are given as

$$\varepsilon^\mu(0, \pm 1) = \begin{pmatrix} 0 \\ \mp\frac{1}{\sqrt{2}} \\ -\frac{i}{\sqrt{2}} \\ 0 \end{pmatrix}, \qquad \varepsilon^\mu(0,0) = \begin{pmatrix} 0 \\ 0 \\ 0 \\ 1 \end{pmatrix}, \quad (B5)$$

where $\varepsilon^\mu(\boldsymbol{p}, \lambda)$ is the general polarization vector (that will be more explicitly discussed further below) with $\boldsymbol{p}$ being the particle momentum and λ its helicity. Taking the absolute square of the invariant amplitude

$$\mathcal{M}_{VPP} = g_{VPP}(p_1 - p_2)_\mu \sum_{\lambda_V = \pm 1, 0} a_{\lambda_V} \varepsilon^\mu(\lambda_V), \quad (B6)$$

yields the general angular distribution which can be expressed as

$$\begin{aligned} |\mathcal{M}|^2 = {}& 2g_{VPP}^2 |\boldsymbol{p}_1|^2 (1 - \rho_{00} + (3\rho_{00} - 1)\cos^2\theta \\ &- 2\text{Re}[\rho_{1-1}]\sin^2\theta \cos 2\phi + 2\text{Im}[\rho_{1-1}]\sin^2\theta \sin 2\phi \\ &- \sqrt{2}\text{Re}[\rho_{10} - \rho_{-10}] \sin 2\theta \cos\phi \\ &+ \sqrt{2}\text{Im}[\rho_{10} + \rho_{-10}] \sin 2\theta \sin\phi), \end{aligned} \quad (B7)$$

where $\rho_{\lambda\lambda'}$ is defined in Eq. (2).

For the $A \to VP$ decay, we also need the polarization vector of the produced vector-meson in the rest frame of the initial axial vector-meson, which is obtained by an inverse Lorentz boost along z-axis followed by an Euler rotation $R(\phi, \theta, 0)$. $R(\alpha, \beta, \gamma)$ here rotates the object about the z-axis by an angle of γ, followed by a rotation around the y-axis by an angle of β, and finally followed by an angle of α around the z-axis. The polarization vectors of the produced vector-meson in the c.m. frame are then obtained as

$$\varepsilon^\mu(\vec{p}, \pm 1) = \begin{pmatrix} 0 \\ \mp\frac{1}{\sqrt{2}}\cos\theta\cos\phi + \frac{i}{\sqrt{2}}\sin\phi \\ \mp\frac{1}{\sqrt{2}}\cos\theta\sin\phi - \frac{i}{\sqrt{2}}\cos\phi \\ \pm\frac{1}{\sqrt{2}}\sin\theta \end{pmatrix},$$

$$\varepsilon^\mu(\vec{p}, 0) = \begin{pmatrix} \frac{|\boldsymbol{p}_1|}{m_1} \\ \frac{E_1}{m_1}\sin\theta\cos\phi \\ \frac{E_1}{m_1}\sin\theta\sin\phi \\ \frac{E_1}{m_1}\cos\theta \end{pmatrix}. \quad (B8)$$

E_1 here is the energy of the produced vector-meson in the c.m. frame. The scalar products between the polarization vectors of the initial axial vector-meson and the final vector-meson are thus calculated as,

$$\varepsilon_{K_1}(1) \cdot \varepsilon_\rho^*(\pm 1) = -\frac{1 \pm \cos\theta}{2} e^{i\phi}, \qquad \varepsilon_{K_1}(-1) \cdot \varepsilon_\rho^*(\pm 1) = -\frac{1 \mp \cos\theta}{2} e^{-i\phi},$$

$$\varepsilon_{K_1}(0) \cdot \varepsilon_\rho^*(\pm 1) = \mp \frac{1}{\sqrt{2}} \sin\theta, \qquad \varepsilon_{K_1}(\pm 1) \cdot \varepsilon_\rho^*(0) = \pm \frac{E_1}{\sqrt{2}m_1} \sin\theta e^{\pm i\phi},$$

$$\varepsilon_{K_1}(0) \cdot \varepsilon_\rho^*(0) = -\frac{E_1}{m_1} \cos\theta. \tag{B9}$$

The general angular distribution is calculated as

$$\mathcal{M}_{K_1 VP}(\lambda_V) = \sqrt{2} m_{K_1} g_{K_1 VP} \sum_{\lambda_{K_1}=\pm 1,0} a_{\lambda_{K_1}} \varepsilon^\mu(\lambda_{K_1}) \varepsilon_\mu^*(\lambda_V), \tag{B10}$$

$$\sum_{\lambda_V=\pm 1,0} |\mathcal{M}_{K_1 VP}(\lambda_V)|^2 = 2m_{K_1}^2 g_{K_1 VP}^2 \Bigg(1 + \frac{p_1^2}{2m_1^2}(1 - \rho_{00} + (3\rho_{00} - 1)\cos^2\theta - 2\mathrm{Re}[\rho_{1-1}]\sin^2\theta\cos 2\phi$$

$$+ 2\mathrm{Im}[\rho_{1-1}]\sin^2\theta\sin 2\phi - \sqrt{2}\mathrm{Re}[\rho_{10} - \rho_{-10}]\sin 2\theta\cos\phi + \sqrt{2}\mathrm{Im}[\rho_{10} + \rho_{-10}]\sin 2\theta\sin\phi) \Bigg). \tag{B11}$$

Additionally, using the scalar product of the polarization vectors of the initial axial vector-meson and the final vector-meson, we obtain the four possible amplitudes depicted in Fig. 4 as follows.

$$|\mathcal{M}_{TT}|^2 = 2m_{K_1}^2 g_{K_1 VP}^2 \sum_{\lambda_{K_1}=\pm 1} \sum_{\lambda_V=\pm 1} |\varepsilon^\mu(\lambda_{K_1})\varepsilon_\mu^*(\lambda_V)|^2 = 2m_{K_1}^2 g_{K_1 VP}^2 (1 + \cos^2\theta),$$

$$|\mathcal{M}_{LT}|^2 = 2m_{K_1}^2 g_{K_1 VP}^2 \sum_{\lambda_{K_1}=0} \sum_{\lambda_V=\pm 1} |\varepsilon^\mu(\lambda_{K_1})\varepsilon_\mu^*(\lambda_V)|^2 = 2m_{K_1}^2 g_{K_1 VP}^2 \sin^2\theta,$$

$$|\mathcal{M}_{TL}|^2 = 2m_{K_1}^2 g_{K_1 VP}^2 \sum_{\lambda_{K_1}=\pm 1} \sum_{\lambda_V=0} |\varepsilon^\mu(\lambda_{K_1})\varepsilon_\mu^*(\lambda_V)|^2 = 2m_{K_1}^2 g_{K_1 VP}^2 \frac{E_1^2}{m_1^2} \sin^2\theta,$$

$$|\mathcal{M}_{LL}|^2 = 2m_{K_1}^2 g_{K_1 VP}^2 \sum_{\lambda_{K_1}=0} \sum_{\lambda_V=0} |\varepsilon^\mu(\lambda_{K_1})\varepsilon_\mu^*(\lambda_V)|^2 = 2m_{K_1}^2 g_{K_1 VP}^2 \frac{E_1^2}{m_1^2} \cos^2\theta. \tag{B12}$$

APPENDIX C: MORE DETAILS ABOUT THE HELICITY FORMALISM

The two-body decay process is considered starting from a definite angular momentum state of $|JM\rangle$ in the mother particle rest frame, decaying into two particle helicity state $|p\phi\theta\lambda\rangle$, where $p = p_1 - p_2$ and $\lambda = \lambda_1 - \lambda_2$ are the relative momenta and helicity difference, respectively, between the two decaying particles denoted with subscripts 1 and 2. The notation and derivation of this section are adapted from Ref. [26].

1. One particle state

First, we study the single-particle canonical and helicity states. The canonical state is defined as a state labeled by its momentum, total angular momentum and its z-component. A general canonical state with arbitrary momentum pointing in the ϕ, θ direction is then constructed by first

inversely rotating the particle such that it aligns with the z-axis, followed by a Lorentz boost in the z-direction, and finally a rotation back into the momentum direction of the particle with polar angles (ϕ, θ),

$$|\vec{p}jm| = U(R(\phi,\theta,0)L_z(p)R^{-1}(\phi,\theta,0))|0jm\rangle, \tag{C1}$$

where $L_z(p)$ is a Lorentz boost along the z-axis. When the particle is at rest, the canonical state transforms under rotation as

$$U(R)|0jm\rangle = \sum_{m'} D^j(R)_{m'm}|0jm'\rangle, \tag{C2}$$

where $D^j(R)_{m'm}$ is a linear representation of a rotation operator $U(R)$ [26].

The helicity state is labeled by the momentum, total angular momentum and helicity. It is similarly constructed

by firstly Lorentz boosting the rest state $|0j\lambda\rangle$ (which is here defined such that λ is the eigenstate of the z-component of the angular momentum, it is thus the same as $|0jm\rangle$ with $m = \lambda$). along the z-axis followed by a rotation such that the momentum points into the direction specified by the polar angles ϕ and θ. We thus have

$$|\vec{p}j\lambda\rangle = U(R(\phi,\theta,0)L_z(p))|0j\lambda\rangle. \qquad (C3)$$

The relation between canonical and helicity states is given as

$$|\vec{p}j\lambda\rangle = U(R(\phi,\theta,0)L_z(p)R^{-1}(\phi,\theta,0))U(R(\phi,\theta,0))|0j\lambda\rangle$$
$$= \sum_m D^j(\phi,\theta,0)_{m\lambda}|\vec{p}jm\rangle \qquad (C4)$$

We here choose our normalization to be Lorentz invariant, such that

$$\langle\vec{p}'j'\lambda'|\vec{p}j\lambda\rangle = (2\pi)^3 2E_{\vec{p}}\delta^3(\vec{p}-\vec{p}')\delta_{jj'}\delta_{\lambda\lambda'},$$
$$\langle\vec{p}'j'm'|\vec{p}jm\rangle = (2\pi)^3 2E_{\vec{p}}\delta^3(\vec{p}-\vec{p}')\delta_{jj'}\delta_{mm'}. \qquad (C5)$$

2. Two particle state

By definition, the two particle helicity state is a tensor product of two one particle states in the c.m. frame,

$$|\phi\theta\lambda_1\lambda_2\rangle = U(R(\phi,\theta,0))[U(L_z(p))|0j_1\lambda_1\rangle$$
$$\otimes U(L_z(-p))|0j_2 -\lambda_2\rangle]. \qquad (C6)$$

We next derive the relation between the two particle helicity state and a state of definite angular momentum $|JM\lambda_1\lambda_2\rangle$. Here, J and M denote the total angular momentum and its projection onto the z-axis of the initial particle, respectively. We assume that the above general two particle helicity state, with the momentum of one particle specified by the angles (ϕ,θ) in the c.m. frame, is related to the total angular momentum state by a coefficient $C_{JM}(\phi,\theta,\lambda_1,\lambda_2)$ as

$$|\phi\theta\lambda_1\lambda_2\rangle = \sum_{JM} C_{JM}(\phi,\theta,\lambda_1,\lambda_2)|JM\lambda_1\lambda_2\rangle. \qquad (C7)$$

Let us here derive an explicit expression for $C_{JM}(\phi,\theta,\lambda_1,\lambda_2)$. The standard helicity state is defined for the state where $\phi = \theta = 0$,

$$|00\lambda_1\lambda_2\rangle = \sum_{JM} C_{JM}(0,0,\lambda_1,\lambda_2)|JM\lambda_1\lambda_2\rangle$$
$$= \sum_J C_{J\lambda}(0,0,\lambda_1,\lambda_2)|J\lambda\lambda_1\lambda_2\rangle, \qquad (C8)$$

In the standard state, particle 2 is heading toward the negative z-direction, thus its projection on the z-axis is

$-\lambda_2$. Therefore, the total angular momentum projection is given by $\lambda = \lambda_1 - \lambda_2$. By a definition of two particle helicity state, it can also be viewed as a state which is rotated from the standard state. Hence,

$$|\phi\theta\lambda_1\lambda_2\rangle = U(R)|00\lambda_1\lambda_2\rangle$$
$$= \sum_J C_{J\lambda}(0,0,\lambda_1,\lambda_2)U(R)|J\lambda\lambda_1\lambda_2\rangle$$
$$= \sum_{JM} C_{J\lambda}(0,0,\lambda_1,\lambda_2)D^J(R)_{M\lambda}|JM\lambda_1\lambda_2\rangle, \qquad (C9)$$

where we have in the last line made use of the fact that a state of definite angular momentum behaves the same way as given in Eq. (C2). Making use of proper orthogonality relations of the states $|\phi\theta\lambda_1\lambda_2\rangle$ and $|JM\lambda_1\lambda_2\rangle$ and properties of the rotation matrix $D^J(R)_{M\lambda}$ (see for example Ref. [26] for more details), we obtain $C_{JM}(0,0,\lambda_1,\lambda_2)$ as

$$C_{JM}(0,0,\lambda_1,\lambda_2) = \sqrt{\frac{2J+1}{4\pi}}, \qquad (C10)$$

and, comparing Eq. (C7) with the last line of Eq. (C9), we finally have

$$C_{JM}(\phi,\theta,\lambda_1,\lambda_2) = \sqrt{\frac{2J+1}{4\pi}}D^J(R)_{M\lambda}, \qquad (C11)$$

where again $\lambda = \lambda_1 - \lambda_2$.

3. Two body decay amplitude

The two body decay amplitude is a transition amplitude from a definite angular momentum state $|JM\rangle$ of the initial particle to a two particle helicity state $|\phi\theta\lambda_1\lambda_2\rangle$ of the daughter particles in the c.m. frame. The transition amplitude from $|JM\rangle$ to $|\phi\theta\lambda_1\lambda_2\rangle$ is given as below,

$$f_{\lambda M} = \langle\phi\theta\lambda_1\lambda_2|H_{\text{int}}|JM\rangle$$
$$= \sum_{J'M'\lambda_1'\lambda_2'} \langle\phi\theta\lambda_1\lambda_2|J'M'\lambda_1'\lambda_2'\rangle\langle J'M'\lambda_1'\lambda_2'|H_{\text{int}}|JM\rangle$$
$$= \sqrt{\frac{2J+1}{4\pi}}D^J(R)^*_{M\lambda}\langle JM\lambda_1\lambda_2|H_{\text{int}}|JM\rangle, \qquad (C12)$$

where Eq. (C11) and angular momentum conservation was used in the second line. H_{int} here stands for the interaction Hamiltonian describing the decay. Making use of the fact that this is a scalar quantity, the matrix element $\langle JM\lambda_1\lambda_2|H_{\text{int}}|JM\rangle$ cannot depend on M, but only on the rotational invariants J, λ_1 and λ_2. We will hence denote it as $\langle JM\lambda_1\lambda_2|H_{\text{int}}|JM\rangle \equiv H^J_{\text{int}}(\lambda_1,\lambda_2)$ in what follows.

If we specify the initial state $|I\rangle$ as superposition of the different M quantum numbers, specifically $|I\rangle = \sum_M a_M|JM\rangle$ and in analogy to Eq. (2) define the spin density matrix as $\rho_{MM'} = a_M a^*_{M'}$, the normalized angular

distribution of this decay can be given as $I(\phi, \theta) = |\sum_M a_M f_{\lambda M}|^2/\Gamma$, where Γ is the decay width of the initial particle. We hence obtain

$$
\begin{aligned}
I(\phi, \theta) &= \frac{1}{\Gamma} \sum_{\lambda_1 \lambda_2} \sum_{MM'} f_{\lambda M} \rho_{MM'} f^*_{\lambda M'} = \frac{1}{\Gamma} \sum_{\lambda_1 \lambda_2} \sum_{MM'} \langle \phi \theta \lambda_1 \lambda_2 | H_{\text{int}} | JM \rangle \rho_{MM'} \langle JM' | H_{\text{int}} | \phi \theta \lambda_1 \lambda_2 \rangle \\
&= \frac{1}{\Gamma} \sum_{\lambda_1 \lambda_2} \sum_{MM'} \frac{2J+1}{4\pi} D^{J\dagger}(\phi, \theta, 0)_{\lambda_M} \rho_{MM'} D^J(\phi, \theta, 0)_{M'\lambda} |H^J_{\text{int}}(\lambda_1, \lambda_2)|^2.
\end{aligned}
\tag{C13}
$$

For the $\rho \to \pi\pi$ decay, only the matrix element $H^1_{\text{int}}(0,0)$ is needed, and the angular decay distribution is therefore automatically fixed only from the rotation matrix $D^1(\phi, \theta, 0)$, given in Eq. (13). As a result, we obtain

$$
\begin{aligned}
I(\phi, \theta) = \frac{3}{8\pi} &(1 - \rho_{00} + (3\rho_{00} - 1)\cos^2\theta - \sqrt{2}\text{Re}[\rho_{10} - \rho_{-10}] \sin 2\theta \cos \phi + \sqrt{2}\text{Im}[\rho_{10} + \rho_{-10}] \sin 2\theta \sin \phi \\
&- 2\text{Re}[\rho_{1-1}]\sin^2\theta \cos 2\phi + 2\text{Im}[\rho_{1-1}]\sin^2\theta \sin 2\phi),
\end{aligned}
\tag{C14}
$$

which agrees with Eq. (6).

On the other hand, for the $K_1 \to \rho K$ decay, the three matrix elements $H^1_{\text{int}}(1,0)$, $H^1_{\text{int}}(0,0)$ and $H^1_{\text{int}}(-1,0)$ need to be considered. Confining us here to strong and thus parity conserving decay, we can make use of the symmetry property of $H^1_{\text{int}}(1,0) = H^1_{\text{int}}(-1,0)$ and are hence left with two independent terms, which have to be determined from a specific interaction Hamiltonian. In this work, it can be easily obtained from the interaction Lagrangian given in Eq. (8) and $H_{\text{int}} = -L_{\text{int}}$. Next, we compute the transition amplitude of Eq. (C12) using the polarization vectors given in Appendix B. To determine the relative strength of the two terms, we only need two independent transition amplitudes, with an outgoing vector particle carrying a different helicity λ_1. Specifically, we have

$$
f_{11} \propto \epsilon^*_\rho(1) \cdot \epsilon_{K_1}(1) = -\frac{1 + \cos\theta}{2} e^{i\phi},
\tag{C15}
$$

and

$$
f_{01} \propto \epsilon^*_\rho(0) \cdot \epsilon_{K_1}(1) = -\frac{E_1}{\sqrt{2}m_1} \sin\theta e^{i\phi}.
\tag{C16}
$$

Comparing this with Eq. (C12), we note that

$$
H^1_{\text{int}}(1,0) = H^1_{\text{int}}(-1,0) \propto g_{K_1\rho K},
\tag{C17}
$$

and

$$
H^1_{\text{int}}(0,0) \propto g_{K_1\rho K} \frac{E_1}{m_1}.
\tag{C18}
$$

This is sufficient to derive the angular distribution of the $K_1 \to \rho K$ decay as

$$
\begin{aligned}
I(\phi, \theta) = \frac{1}{\Gamma} \frac{3}{4\pi} &\Bigg(|H(1,0)|^2 + \frac{1}{2}(|H(0,0)|^2 - |H(1,0)|^2) \\
&\times (1 - \rho_{00} + (3\rho_{00} - 1)\cos^2\theta - \sqrt{2}\text{Re}[\rho_{10} - \rho_{-10}] \sin 2\theta \cos \phi + \sqrt{2}\text{Im}[\rho_{10} + \rho_{-10}] \sin 2\theta \sin \phi \\
&- 2\text{Re}[\rho_{1-1}]\sin^2\theta \cos 2\phi + 2\text{Im}[\rho_{1-1}]\sin^2\theta \sin 2\phi) \Bigg) \\
= \frac{3}{4\pi(3 + \frac{p_1^2}{m_1^2})} &\Bigg(1 + \frac{p_1^2}{2m_1^2}(1 - \rho_{00} + (3\rho_{00} - 1)\cos^2\theta - \sqrt{2}\text{Re}[\rho_{10} - \rho_{-10}] \sin 2\theta \cos \phi \\
&+ \sqrt{2}\text{Im}[\rho_{10} + \rho_{-10}] \sin 2\theta \sin \phi - 2\text{Re}[\rho_{1-1}]\sin^2\theta \cos 2\phi + 2\text{Im}[\rho_{1-1}]\sin^2\theta \sin 2\phi) \Bigg),
\end{aligned}
\tag{C19}
$$

which agrees with Eq. (10).

[1] Y. Nambu and G. Jona-Lasinio, Phys. Rev. **122**, 345 (1961).
[2] Y. Nambu and G. Jona-Lasinio, Phys. Rev. **124**, 246 (1961).
[3] T. Hatsuda and T. Kunihiro, Phys. Rev. Lett. **55**, 158 (1985).
[4] G. E. Brown and M. Rho, Phys. Rev. Lett. **66**, 2720 (1991).
[5] T. Hatsuda and S. H. Lee, Phys. Rev. C **46**, R34 (1992).
[6] S. Leupold, V. Metag, and U. Mosel, Int. J. Mod. Phys. E **19**, 147 (2010).
[7] For review see, R. S. Hayano and T. Hatsuda, Rev. Mod. Phys. **82**, 2949 (2010).
[8] M. Ichikawa *et al.*, Acta Phys. Pol. B Proc. Suppl. **16**, A143 (2023).
[9] V. Metag, M. Nanova, and E. Y. Paryev, Prog. Part. Nucl. Phys. **97**, 199 (2017).
[10] H. Ohnishi, F. Sakuma, and T. Takahashi, Prog. Part. Nucl. Phys. **113**, 103773 (2020).
[11] P. Salabura and J. Stroth, Prog. Part. Nucl. Phys. **120**, 103869 (2021).
[12] K. Aoki *et al.*, Few-Body Syst. **64**, 63 (2023).
[13] H. Sako *et al.*, P88: Study of in-medium modification of ϕ mesons inside the nucleus with $\phi \to K^+ K^-$ measurement with the E16 spectrometer, https://j-parc.jp/researcher/Hadron/en/pac_2107/pdf/P88_2021-12.pdf.
[14] P. Gubler, E. Bratkovskaya, M. Ichikawa, and T. Song, EPJ Web Conf. **291**, 04003 (2024).
[15] S. H. Lee, JPS Conf. Proc. **26**, 011012 (2019).
[16] T. Song, T. Hatsuda, and S. H. Lee, Phys. Lett. B **792**, 160 (2019).
[17] S. H. Lee, Symmetry **15**, 799 (2023).
[18] S. H. Lee, Phys. Rev. C **57**, 927 (1998); **58**, 3771(E) (1998).
[19] H. Kim and P. Gubler, Phys. Lett. B **805**, 135412 (2020).
[20] I. W. Park, H. Sako, K. Aoki, P. Gubler, and S. H. Lee, Phys. Rev. D **107**, 074033 (2023).
[21] H. S. Sung, S. Cho, J. Hong, S. H. Lee, S. Lim, and T. Song, Phys. Lett. B **819**, 136388 (2021).
[22] R. L. Workman *et al.* (Particle Data Group), Prog. Theor. Exp. Phys. **2022**, 083C01 (2022).
[23] K. Schilling, P. Seyboth, and G. E. Wolf, Nucl. Phys. **B15**, 397 (1970); **B18**, 332(E) (1970).
[24] Eugene Wigner, *Gruppentheorie und ihre Anwendung auf die Quantenmechanik der Atomspektren* (Vieweg Verlag, Braunschweig, 1931), 10.1007/0-306-47123-x.
[25] E. Leader, Cambridge Monogr. Part. Phys Nucl. Phys. Cosmol. **15**, 1 (2023).
[26] S. U. Chung, Spin formalisms, Report No. CERN-71-08, 10.5170/CERN-1971-008 (1971).
[27] V. Devanathan, *Angular Momentum Techniques in Quantum Mechanics* (Springer, Netherlands, 2005).